*Journal of Nano- and Electronic Physics*
Vol. **18** No 4, 04001(11pp) (2026)

*Журнал нано- та електронної фізики*
Том **18** № 4, 04001(11cc) (2026)

OPEN ACCESS

## REGULAR ARTICLE

# Theory of Dipole-Exchange Spin Waves in a Ferromagnetic Nanotube in the Presence of a Thermoelectrically Induced Spin-Transfer Torque. Elliptic Nanotube Case

V.V. Kulish* ✉, S.I. Yeromin

*National Technical University of Ukraine «Igor Sikorsky Kyiv Polytechnic Institute», 03056 Kyiv, Ukraine*

(Received 04 April 2026; revised manuscript received 19 August 2026; published online 21 August 2026)

A theoretical model of linear dipole-exchange spin waves in a conducting ferromagnetic (easy-axis ferromagnet) nanotube with an elliptic cross-section subjected to an axial temperature gradient is developed. The temperature gradient generates a thermoelectric spin-polarized current, whose action on magnetization dynamics is described by Zhang–Li spin-transfer torque terms. Exchange interaction, dipole-dipole interaction, uniaxial anisotropy and Gilbert damping are taken into account within the linearized Landau–Lifshitz–Gilbert equation and the magnetostatic approximation. The corresponding dispersion relation is derived. It is shown that the thermally induced spin current produces a Doppler-type shift of the real part of the spin-wave frequency and modifies the effective damping through the nonadiabatic spin-transfer contribution. The condition of spin-wave excitation is obtained. The ellipticity of the cross-section affects the spectrum through transverse quantization: the fundamental mode remains identical to that of a circular nanotube, whereas nonzero transverse modes are described by Mathieu functions in elliptic cylindrical coordinates. Implicit expression for the transverse wavenumber has been found and (for a nanotube close to a circular one) simplified into an explicit asymptotic expression for the ellipticity-induced correction to the transverse wavenumber. The leading effect of ellipticity is shown to be splitting of the transverse doublet for the first mode, while higher modes acquire no first-order wavenumber shift in this approximation. The results demonstrate that the temperature gradient controls longitudinal propagation and damping, whereas ellipticity provides an additional geometrical mechanism for tuning transverse spin-wave modes in nanoscale magnonic and spin-caloritronic devices.

**Keywords:** Spin wave, Nanomagnetism, Dipole-exchange theory, Mode splitting, Thermoelectricity, Spin transfer.

DOI: 10.21272/jnep.18(4).04001

PACS numbers: 75.30.Ds, 75.75.a, 73.50.Lw, 75.76. + j, 75.30.Gw

## 1. INTRODUCTION

Spin-wave dynamics in magnetic nanostructures is one of the central subjects of modern nanomagnetism, since magnons can transport phase and angular-momentum information without requiring a net mass transfer of magnetic material. In nanoscale ferromagnets, the properties of spin waves are governed not only by the intrinsic material parameters, but also by the shape and characteristic dimensions of the magnetic body [1-4]. When at least one dimension of a system becomes comparable with the exchange length, the exchange interaction and the dipole-dipole interaction must be treated on equal footing, while the boundary conditions imposed by the nanoscale geometry become an essential part of the spectral problem. This makes magnetic nanotubes and related curvilinear structures especially relevant objects for magnonics, because their spectra are simultaneously affected by axial propagation, finite wall thickness, surface curvature, and transverse quantization.

Ferromagnetic nanotubes form a specific class of quasi-one-dimensional nanosystems. Compared with solid nanowires, nanotubes possess additional geometrical parameters, such as inner radius and wall thickness, which provide extra possibilities for tuning spin-wave spectra and can broaden the operating range of corresponding nanoscale magnonic devices. Magnetic nanotubes and rolled-up magnetic nanomembranes have been considered in the context of nanomagnetism, biomedical applications, domain-wall motion, and curvilinear magnetic effects [5-8]. At the same time, their spin-wave properties remain less systematically studied than those of films, stripes, or planar multilayers, especially when the exchange contribution, dipolar fields, damping, and current-induced torques are included simultaneously.

Non-circularity of the cross-section and ellipticity in particular, introduces an additional geometrical degree of freedom into the set of parameters controlling the spin-wave spectrum of a nanotube. This makes it possible to tune the transverse mode structure without changing the material composition or the nanotube length. Since nanotubes with non-circular (in particular, elliptic) cross-sections are experimentally realizable [5, 9, 10], elliptic ferromagnetic nanotubes constitute a physically relevant platform for theoretical studies aimed at extending the operating range of spin-wave-based nanoscale devices. Moreover, for real nanotubes

* Correspondence e-mail: s.yeromin.ua@gmail.com





Cite this article as: V.V. Kulish et al., *J. Nano- Electron. Phys.* 18 No 4, 04001 (2026) https://doi.org/10.21272/jnep.18(4).04001

that have cross-section close to circular, different factors (fabrication processes, mechanical stresses, substrate effects, self-rolling of magnetic nanomembranes etc.) lead to deviations from a perfectly circular shape, making the elliptic cross-section model, in general case, more precise for them than the circular cross-section model. The ellipticity is expected to affect primarily the transverse mode structure and the allowed values of the orthogonal wave number.

Spin waves in ferromagnetic nanotubes of circular and elliptic cross-sections have been investigated previously by the authors in several limiting cases. For a circular nanotube, dipole-exchange spin waves without thermoelectric driving were studied within the magnetostatic approach [11]. Later, spin waves in a ferromagnetic nanotube of elliptic cross-section were analyzed in the presence of an externally introduced spin-polarized electric current; in that case the spin-transfer action was described by the Slonczewski-Berger torque, and the transverse spectrum was obtained in terms of Mathieu functions [12]. More recently, a theory of dipole-exchange spin waves in a circular ferromagnetic nanotube subjected to an axial temperature gradient was developed by Kulish and Yeromin [13]. In that paper, the temperature gradient generated a thermoelectric current through the Seebeck effect; because the current in a conducting ferromagnet is spin-polarized, it produced a spin-transfer torque of Zhang-Li type. It was shown that such a thermoelectrically induced spin current shifts the real part of the spin-wave frequency and changes the effective damping, thus creating conditions for spin-wave amplification or generation.

The present work extends this thermally driven problem from a circular nanotube to a nanotube with an elliptic cross-section. The aim of this paper is to develop a linear dipole-exchange theory of spin waves in a uniaxial ferromagnetic nanotube of elliptic cross-section in the presence of an axial temperature gradient. The magnetization dynamics is described by the linearized Landau-Lifshitz-Gilbert equation supplemented with Zhang-Li spin-transfer torques. Exchange interaction, dipole-dipole interaction, uniaxial anisotropy, and damping are taken into account. Using the magnetostatic approximation and elliptic cylindrical coordinates, the equation for the magnetic potential is derived, the corresponding dispersion relation is obtained and the transverse wave-number spectrum is analyzed. Special attention is paid to the comparison with the circular nanotube: the fundamental mode is shown to retain the circular-tube form, whereas the ellipticity manifests itself through the transverse eigenmodes and the associated spectral shifts.

## 2. PROBLEM STATEMENT

Let us consider a long one-layer conducting ferromagnetic nanotube with an elliptic cross-section. The nanotube length is assumed to be much larger than its transverse dimensions; therefore, the system may be treated as translationally invariant along its axis. This axis is chosen as the $Oz$ axis of the coordinate system. The inner and outer surfaces of the nanotube are taken to be confocal elliptic cylinders, which can be described as surfaces $u$ = const in elliptic cylindrical coordinates $(u, v, z)$

$$x = f\cosh u\cos v\,,\ \ y = f\sinh u\sin v\,,\ \ z = z,$$

where $f$ is the focal parameter. The inner and outer boundaries correspond to $u = u_1$ and $u = u_2$, respectively. Thus, the ellipticity of the cross-section enters the problem through the geometrical parameters $u_1, u_2$, or, equivalently, through the ratios of the corresponding semiaxes ($b_1 = f\cosh u_1$, $a_1 = f\sinh u_1$ for the internal boundary and $b_2 = f\cosh u_2$, $a_2 = f\sinh u_2$ for the outer boundary).

The nanotube is assumed to be composed of a uniaxial ferromagnet of the easy-axis type. The anisotropy axis is directed along the nanotube axis. An external homogeneous magnetic field $\mathbf{H}_0^{(e)}$ is also applied along $Oz$. Under these conditions, the equilibrium magnetization is taken to be uniform and directed along the same axis: $\mathbf{M}_0 = M_0\mathbf{e}_z$. The ferromagnet is characterized by the exchange constant $\alpha$, the uniaxial anisotropy parameter $\beta$, the equilibrium magnetization $M_0$, the gyromagnetic ratio $\gamma$, and the Gilbert damping parameter $\alpha_G$. A stationary temperature gradient $\nabla T = \frac{\partial T}{\partial z}\mathbf{e}_z$ is applied along the nanotube axis, see Fig. 1.

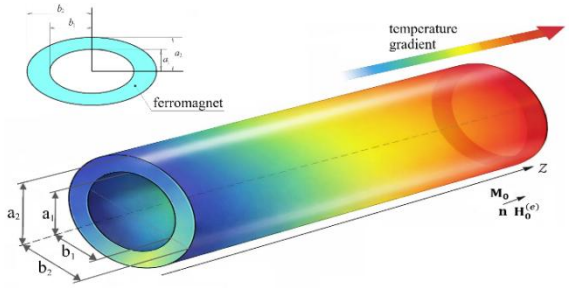


**Fig. 1** – Nanotube investigated in the paper

Analogously to the previous paper by the authors [13], this gradient produces a thermoelectric current in the conducting ferromagnet. Since the charge transport in a ferromagnet is spin dependent, the induced current is spin-polarized and affects the magnetization dynamics through the bulk spin-transfer mechanism. Without repeating the detailed thermoelectric transport analysis given in [13], let us use its effective result: after applying two-current model in the short-circuit approximation, the thermally induced current is represented by the spin-drift velocity

$$\boldsymbol{v_s} = v_s\mathbf{e}_z = \frac{\mu_B P}{eM_0}j_z\mathbf{e}_z,$$

where $P$ is the degree of spin polarization of the thermoelectric current and $j_z$ is the axial charge-current density generated by the temperature gradient. In the considered approximation one may write

$$j_z = -\sigma S\frac{\partial T}{\partial z},$$

where $\sigma$ and $S$ are the effective electrical conductivity and Seebeck coefficient of the ferromagnet (the current is generated via Seebeck effect [14, 15]). The magnetic self-field of this current is assumed to be small compared with the external and anisotropy fields and is therefore neglected. Purely magnon spin current generated by the temperature gradient (spin Seebeck effect) can also be neglected for typical thin metallic nanotubes with high electrical conductivity, moderate

thermoelectric spin polarization, and weak axial nonuniformity of the magnon subsystem [13].

Let us study small-amplitude spin waves propagating along the nanotube axis. The magnetization and the internal magnetic field $\mathbf{H}^{(i)}$, then, can be written as

$$\mathbf{M} = \mathbf{M}_0 + \mathbf{m},\ \mathbf{H}^{(i)} = \mathbf{H}_0^{(i)} + \mathbf{h}, \qquad (1)$$

where $|\,\mathbf{m}\,| \ll M_0, |\,\mathbf{h}\,| \ll |\,\mathbf{H}_0^{(i)}\,|$ and $\mathbf{H}_0^{(i)}$ is the equilibrium internal magnetic field inside the tube wall. Thus, the linearized theory of spin waves can be used. The perturbations are assumed to be harmonic in time and along the nanotube axis:

$$\mathbf{m}(\mathbf{r},t) = \mathbf{m}_0(u,v)\exp[i(\omega t - k_\parallel z)],$$

$$\mathbf{h}(\mathbf{r},t) = \mathbf{h}_0(u,v)\exp[i(\omega t - k_\parallel z)].$$

Since the transverse dimensions of the nanotube are nanoscale, the exchange interaction can influence significantly the spin wave pattern and thus, must be considered together with the magnetic dipole-dipole interaction.

In a conducting ferromagnet subjected to a temperature gradient, the Seebeck current is generally spin-dependent, so the charge flow is accompanied by a spin-polarized component. The coupling of such a current to a spatially nonuniform magnetization is naturally described by the Zhang-Li spin-transfer terms [16]. The adiabatic term produces a drift-like correction to the spin-wave dispersion, usually interpreted as a current-induced Doppler shift [17, 18], whereas the nonadiabatic term enters the dissipative part of the dynamics and may either enhance or compensate Gilbert damping.

The main task of the present work is to develop a theoretical description of the above spin waves, derive the equation for the magnetic potential, obtain the corresponding dispersion relation, and analyze the transverse wavenumber spectrum. In contrast to the circular nanotube, the transverse part of the problem is governed by elliptic boundary conditions, leading to a modified spectrum of transverse wave numbers. At the same time, the longitudinal propagation mechanism remains analogous to that in the circular nanotube considered by the authors in the earlier paper [13].

## 3. SYSTEM OF EQUATIONS FOR A SPIN WAVE

In order to describe the investigated spin waves in the elliptic ferromagnetic nanotube, let us use the Landau–Lifshitz–Gilbert equation

$$\frac{\partial \mathbf{M}}{\partial t} = \gamma[\mathbf{M} \times \mathbf{H}_{\text{eff}}] + \frac{\alpha_G}{M_0}\left[\mathbf{M} \times \frac{\partial \mathbf{M}}{\partial t}\right]$$

with the effective magnetic field acting on the magnetization

$$\mathbf{H}_{\text{eff}} = \mathbf{H}^{(i)} + \alpha\Delta\mathbf{M} + \beta\mathbf{n}(\mathbf{M}\mathbf{n}),$$

here $\alpha$ is the exchange constant, $\beta$ is the uniaxial anisotropy parameter, and $\mathbf{n} = \mathbf{e}_z$ is the unit vector directed along the anisotropy axis. Influence of the temperature gradient will be accounted through the Zhang-Li spin-transfer torque

$$\mathbf{T}_{\text{ZL}} = -(\boldsymbol{v_s}\nabla)\mathbf{M} + \frac{\xi}{M_0}[\mathbf{M} \times (\boldsymbol{v_s}\nabla)\mathbf{M}],$$

where $\xi$ is the nonadiabaticity parameter. This form of the torque is appropriate for a conducting one-layer ferromagnet, where the spin-polarized current is generated inside the magnetic material itself and flows along the equilibrium magnetization direction. The current is induced by the axial temperature gradient, while the detailed thermoelectric mechanism has been discussed in the earlier paper by the authors [13] and will not be repeated here.

Let us linearize this equation (with the magnetization and magnetic field represented according to (1)). After considering that in the linear approximation one has $\mathbf{m}\mathbf{e}_z = 0$ (so the spin-wave magnetization is transverse to the equilibrium magnetization), and that for a sufficiently long nanotube (magnetized along its axis) the equilibrium demagnetizing field in the axial direction may be neglected ($\mathbf{H}_0^{(i)} = \mathbf{H}_0^{(e)} = H_0^{(e)}\mathbf{e}_z$), the linearized equation for the magnetization perturbation takes the form

$$\frac{\partial \mathbf{m}}{\partial t} + v_s\frac{\partial \mathbf{m}}{\partial z} = \gamma M_0\left[\mathbf{e}_z \times \left(\mathbf{h} + \alpha\Delta\mathbf{m} - \left(\beta + \frac{H_0^{(e)}}{M_0}\right)\mathbf{m} + \frac{\alpha_G}{\gamma M_0}\frac{\partial \mathbf{m}}{\partial t}\right)\right] + \xi v_s\left[\mathbf{e}_z \times \frac{\partial \mathbf{m}}{\partial z}\right].$$

For spin waves propagating along the nanotube axis

$$\mathbf{m}(\mathbf{r},t) = \mathbf{m}_0(u,v)\exp[i(\omega t - k_\parallel z)],$$

$$\mathbf{h}(\mathbf{r},t) = \mathbf{h}_0(u,v)\exp[i(\omega t - k_\parallel z)],$$

the linearized equation becomes

$$i(\omega - v_s k_\parallel)\mathbf{m}_0 = \gamma M_0\left[\mathbf{e}_z \times \left(\mathbf{h}_0 + \alpha\Delta\mathbf{m}_0 - \tilde{\beta}\,\mathbf{m}_0\right)\right], \quad (2)$$

Where

$$\tilde{\beta} = \beta + \frac{H_0^{(e)}}{M_0} - \frac{i}{\gamma M_0}(\alpha_G\omega - \xi v_s k_\parallel).$$

This form explicitly separates the two effects of the thermoelectrically induced spin current. The adiabatic Zhang-Li term changes the frequency through the replacement $\omega \to \omega - v_s k_\parallel$ (current-induced Doppler shift), whereas the nonadiabatic term enters the imaginary part of the effective magnetic parameter $\tilde{\beta}$ and therefore modifies the damping.

To close the system of equations, let us use the magnetostatic approximation. The magnetic field of the spin wave is expressed through the scalar magnetic potential $\mathbf{h} = -\nabla\Phi$, so Maxwell's equation for the magnetostatic field gives

$$\Delta\Phi - 4\pi\,\text{div}\,\mathbf{m} = 0.$$

For harmonic perturbations this relation becomes

$$\Delta\Phi_0 - 4\pi\,\text{div}\,\mathbf{m}_0 = 0, \qquad (3)$$

Where

$$\Phi(\mathbf{r},t) = \Phi_0(u,v,z)\exp(i\omega t).$$

Thus, the spin-wave problem is reduced to the coupled system (2), (3). These equations form the starting point for deriving the equation for the magnetic potential. The elliptic cross-section enters through the transverse part of the Laplace operator and through the boundary conditions at $u = u_1$ and $u = u_2$, while the temperature gradient enters through the drift velocity $u$ and modifies the longitudinal propagation and effective damping of the spin wave.

## 4. EQUATION FOR THE MAGNETIC POTENTIAL AND ITS SOLUTION

Let us derive the equation for the magnetic potential of the investigated dipole-exchange spin wave in the elliptic nanotube. After substituting (3) into (2) and taking into account $\mathbf{h_0} = -\nabla\Phi_0$, $j_z = -\sigma S\frac{\partial T}{\partial z}$, one can repeat a set of transformations analogous to the ones used in the earlier papers by the authors (e.g., [13]), obtaining

$$\left[\frac{(\omega - v_s k_\parallel)^2}{\gamma^2 M_0^2} - (\tilde{\beta} - \alpha\Delta)(4\pi + \tilde{\beta} - \alpha\Delta)\right]\Delta\Phi_0 + 4\pi(\tilde{\beta} - \alpha\Delta)\frac{\partial^2\Phi_0}{\partial z^2} = 0 \quad (4)$$

This equation is the required equation for the magnetic potential of the spin wave. It has the same general operator structure as in the circular nanotube considered previously, but the transverse part of the Laplace operator must now be written in above-introduced elliptic cylindrical coordinates ($u$, $v$, $z$) with the focal parameter $f$.

In these coordinates, $\Delta = \Delta_\perp + \frac{\partial^2}{\partial z^2}$, where

$$\Delta_\perp = \frac{1}{f^2(\sinh^2 u + \sin^2 v)}\left(\frac{\partial^2}{\partial u^2} + \frac{\partial^2}{\partial v^2}\right).$$

The magnetic potential can be sought in the form

$$\Phi_0(u, v, z) = F(u, v)\exp(-ik_\parallel z),$$

where $k_\parallel$ is the longitudinal wave number. The transverse function $F(u, v)$ is an eigenfunction of the two-dimensional Helmholtz equation in elliptic cylindrical coordinates,$\Delta_\perp F = -k_\perp^2 F$.

Therefore, $\Delta\Phi_0 = -k^2\Phi_0$, where the total wave-number $k^2 = k_\parallel^2 + k_\perp^2$.

The corresponding transverse solutions $F(u, v)$ can be expressed through a combination of Mathieu functions, so

$$\Phi_0(u, v, z) = \left(C_1\,\mathrm{Ce}_m(u, q)\,\mathrm{ce}_m(v, q) + C_2\,\mathrm{Se}_m(u, q)\,\mathrm{se}_m(v, q)\right)\exp(-ik_\parallel z), \quad (5)$$

where $C_1$, $C_2$ are constants, $\mathrm{Ce_m}$, $\mathrm{ce_m}$, $\mathrm{Se_m}$, and $\mathrm{se_m}$ are the Mathieu functions of the order $m$, $m$ is the transverse mode number and $q = \frac{f^2 k_\perp^2}{4}$.

The allowed values of $k_\perp$are determined by the boundary conditions at the inner and outer nanotube surfaces $u = u_1$and $u = u_2$.

These equations show explicitly how the geometry of the elliptic cross-section enters the theory. The longitudinal propagation and the thermally induced spin-transfer effects are contained in $\omega - v_s k_\parallel$ and $\tilde{\beta}$, whereas the ellipticity affects the problem through the transverse operator $\Delta_\perp$(and, consequently, transverse solutions $F(u, v)$ expressed through the Mathieu functions) and the boundary conditions at $u = u_1$and $u = u_2$. Thus, the transition from a circular to an elliptic nanotube changes the transverse eigenvalue problem, while preserving the general form of the dipole-exchange magnetic-potential equation.

## 5. DISPERSION RELATION AND CONDITION OF SPIN-WAVE EXCITATION

Substitution of the solution (5) into the equation for the magnetic potential (4) gives the dispersion equation in the form

$$\left[\frac{(\omega - v_s k_\parallel)^2}{\gamma^2 M_0^2} - (\tilde{\beta} + \alpha k^2)(4\pi + \tilde{\beta} + \alpha k^2)\right]k^2 + 4\pi(\tilde{\beta} + \alpha k^2)k_\parallel^2 = 0 \quad (6)$$

where the sign convention is chosen so that a positive imaginary part of $\omega$ corresponds to damping for the time dependence $\exp(i\omega t)$. Eq. (6) is the sought dispersion equation for dipole-exchange spin waves in an elliptic nanotube in the presence of a thermoelectrically induced spin-polarized current.

Let us introduce

$$\beta_0 = \beta + \frac{H_0^{(e)}}{M_0}.$$

In the absence of damping and nonadiabatic spin-transfer contribution, Eq. (6) gives the real-frequency branch

$$\omega_0 = v_s k_\parallel + \gamma M_0\sqrt{(\beta_0 + \alpha k^2)\left(\beta_0 + \alpha k^2 + 4\pi\frac{k_\perp^2}{k^2}\right)}. \quad (7)$$

The first term in Eq. (3) is the Doppler-type shift caused by the adiabatic Zhang–Li torque. The second term is the ordinary dipole-exchange frequency, modified by the finite transverse wave number. It corresponds to the previous papers by the authors that investigate spin waves in a nanotube without consideration of dissipation and spin current (see, e.g., [11]) Thus, the ellipticity affects the dispersion relation indirectly, through the values of $k_\perp$ determined by the elliptic boundary-value problem.

For typical nanosystems in which periodic spin waves can be excited, both damping and nonadiabaticity can be considered weak: $\alpha_G \ll 1$, $\xi \ll 1$. Retaining only terms linear in $\alpha_G$ and $\xi$, we can obtain from (6) for the real and imaginary parts of the spin wave frequency (writing $\omega = \omega_r + i\omega_i$, with $\omega_r = Re\omega$ and $\omega_i = Im\omega$):

$$\omega_r = v_s k_\parallel + \gamma M_0\sqrt{(\beta_0 + \alpha k^2)\left(\beta_0 + \alpha k^2 + 4\pi\frac{k_\perp^2}{k^2}\right)}, \quad (8)$$

for the positive-frequency branch (the same expression as in the absence of damping and nonadiabatic spin-transfer contribution (7)), and

$$\omega_i = \frac{\beta_0 + \alpha k^2 + 2\pi\frac{k_\perp^2}{k^2}}{\sqrt{(\beta_0 + \alpha k^2)\left(\beta_0 + \alpha k^2 + 4\pi\frac{k_\perp^2}{k^2}\right)}} * \left[\alpha_G\gamma M_0\sqrt{(\beta_0 + \alpha k^2)\left(\beta_0 + \alpha k^2 + 4\pi\frac{k_\perp^2}{k^2}\right)} - (\xi - \alpha_G)v_s k_\parallel\right], \quad (9)$$

with

$$v_s = -\frac{\mu_B P\sigma S}{eM_0}\frac{\partial T}{\partial z}. \quad (10)$$

Eq. (8) shows that the adiabatic spin-transfer torque shifts the real part of the spin-wave frequency. Eq. (9) shows that the nonadiabatic torque changes the effective damping. Depending on the sign and magnitude of $v_s k_\parallel$, the temperature-gradient-induced current may either increase or decrease the attenuation of the spin wave.

Analogously to [13], the condition of compensation of intrinsic damping is obtained from $\omega_i = 0$. Since the prefactor in Eq. (9) is positive, this condition reduces to

$$(\xi - \alpha_G)v_s k_\parallel = \alpha_G\gamma M_0\sqrt{(\beta_0 + \alpha k^2)\left(\beta_0 + \alpha k^2 + 4\pi\frac{k_\perp^2}{k^2}\right)}$$

If

$$(\xi-\alpha_G)v_s k_\parallel > \alpha_G\gamma M_0\sqrt{(\beta_0+\alpha k^2)\left(\beta_0+\alpha k^2+4\pi\frac{k_\perp^2}{k^2}\right)} \quad (11)$$

then $\omega_i < 0$, and the spin-wave amplitude increases with time. This corresponds to spin-wave excitation by the thermoelectrically induced spin-polarized current. If the opposite inequality is fulfilled, the wave attenuates.

Substituting (10), one obtains the threshold temperature gradient

$$\left(\frac{\partial T}{\partial z}\right)_{\rm cr} = -\frac{eM_0\alpha_G\gamma M_0}{\mu_B P\sigma S(\xi-\alpha_G)k_\parallel} * \sqrt{(\beta_0+\alpha k^2)\left(\beta_0+\alpha k^2+4\pi\frac{k_\perp^2}{k^2}\right)} \quad (12)$$

The sign of this gradient must be chosen so that the induced spin drift compensates the Gilbert damping. Eq. (12) also shows that spin-wave excitation is impossible for $k_\parallel = 0$, because the bulk Zhang-Li torque acts through spatial variation of the magnetization along the current direction.

For the fundamental transverse mode $k_\perp = 0$, $k = k_\parallel$, Eqs. (8) and (9) reduce to

$$\omega_r = v_s k_\parallel + \gamma M_0(\beta_0+\alpha k_\parallel^2),$$

$$\omega_i = \alpha_G\gamma M_0(\beta_0+\alpha k_\parallel^2) - (\xi-\alpha_G)v_s k_\parallel.$$

These expressions coincide with the corresponding result for a circular nanotube. Therefore, the ellipticity of the cross-section does not modify the fundamental spin-wave branch in the adopted approximation. Its influence appears through nonzero transverse modes, for which $k_\perp \neq 0$ and the allowed values of $k_\perp$ are determined by the elliptic geometry of the nanotube.

## 6. TRANSVERSE WAVENUMBER SPECTRUM

Let us now determine the spectrum of the transverse, or orthogonal, wave number $k_\perp$. The dispersion relation obtained above contains both the longitudinal component $k_\parallel$ and the transverse component $k_\perp$. Since the nanotube is assumed to be long compared with its transverse dimensions, $k_\parallel$ may be treated as a quasi-continuous variable. In contrast, the transverse motion is confined by the inner and outer boundaries of the nanotube, so the allowed values of $k_\perp$ form a discrete spectrum.

In the present problem, the temperature-gradient-induced spin current enters the equation of motion through the bulk Zhang-Li terms. These terms produce the Doppler-type shift of the real part of the frequency and modify the effective damping, but they do not change the form of the magnetostatic boundary conditions at the nanotube surfaces. Therefore, the transverse quantization is determined by the same type of boundary-value problem as in a nanotube without thermoelectric driving, while the temperature gradient enters the final spin-wave spectrum through the dispersion relation.

In the general case, the transverse wavenumber spectrum is determined by matching the magnetic potential inside the ferromagnetic tube with the potential in the inner and outer nonmagnetic regions. At each ferromagnet-nonmagnet interface one has to impose the standard magnetostatic boundary conditions for the magnetic field, from which the following conditions for the magnetic potential imply:

$$\Phi^{(i)} = \Phi^{(e)},$$

$$(\nabla\Phi)_\tau^{(i)} = (\nabla\Phi)_\tau^{(e)},$$

$$(\partial\Phi/\partial n)^{(i)} - (\partial\Phi/\partial n)^{(e)} = 4\pi \mathrm{m}_n \quad (13)$$

where the superscripts $(i)$ and $(e)$ denote the internal and external regions, respectively, while $n$ and $\tau$ denote the normal and tangential components at the interface.

Let us apply pinned boundary conditions. For such conditions, $\mathbf{m_0}$=0 on both nanotube surfaces and, then, the third relation in (13) can be rewritten as $(\partial\Phi_0/\partial n)^{(i)} = (\partial\Phi_0/\partial n)^{(e)}$ on both nanotube surfaces. (Note that this transverse-spectrum calculation with pinned boundary conditions applies only to nonzero transverse modes, while the fundamental mode $k_\perp = 0$ is treated separately within the thin-wall/uniform-mode approximation.)

Thus, the exact transverse spectrum is obtained from the matching of the internal and external solutions on the inner and outer elliptic surfaces ($u$=$u_1$, $u$=$u_2$). This procedure gives an implicit spectral equation for $k_\perp$. For a circular nanotube the corresponding equation is written in terms of Bessel and Neumann functions. For an elliptic nanotube, the analogous problem is described by Mathieu functions.

Analysis shows that in a general case, more complex boundary conditions should be used to determine the transverse spin wave spectrum (as the angular and radial parts are coupled through the same Mathieu parameter $q$). However, the above-given set of conditions is applicable if the condition $ch2u_1 >> 1 + k_\perp^2/k_{||}^2$ fulfils, which takes place either for longitudinally short waves ($k_{||}$>>$k_\perp$) or for a cross-section close to circular ($b_1$-$a_1$/$a_1$<<1, $b_2$-$a_2$/$a_2$<<1), for which $u_1$is large. Then, the sought spectrum is defined by the real roots of the following implicit relation:

$$\frac{Ce_m'(u_1,q)F_m^+(u_1,k_{||}) - Ce_m(u_1,q)F_m^{+\prime}(u_1,k_{||})}{Se_m'(u_1,q)F_m^+(u_1,k_{||}) - Se_m(u_1,q)F_m^{+\prime}(u_1,k_{||})} =$$
$$= \frac{Ce_m'(u_2,q)F_m^-(u_2,k_{||}) - Ce_m(u_2,q)F_m^{-\prime}(u_2,k_{||})}{Se_m'(u_2,q)F_m^-(u_2,k_{||}) - Se_m(u_2,q)F_m^{-\prime}(u_2,k_{||})},$$

with the functions

$$F_m^\pm(u,k_{||}) = Ce_m\left(u,\frac{-k_{||}^2f^2}{4}\right) \pm iSe_m\left(u,\frac{-k_{||}^2f^2}{4}\right).$$

The following calculation is performed for a separable confocal-elliptic model, in which the inner and outer nanotube surfaces are described by u = $u_1$and u = $u_2$.

Let us analyze the obtained implicit relation for the transverse wavenumber spectrum. For nanotubes with an elliptic cross-section close to a circular one ($b_1$-$a_1$/$a_1$<<1, $b_2$-$a_2$/$a_2$<<1) that are also thin-walled ($a_2$-$a_1$/$a_1$<<1, $b_2$-$b_1$/$b_1$<<1) the transverse spin wave spectrum becomes close to a quasi-one-dimensional (analogously to the case of a circular nanotube [13])

$$k_\perp = \frac{\pi n}{d},\ n = 1,2,3,\ldots, \quad (14)$$

with the mean nanotube thickness

$$d = \frac{f}{2}(exp(u_2) - exp(u_1)).$$

As it has already been mentioned earlier, fundamental mode also exists for the investigated nanotube configuration (corresponding to $n$=0 in the above relation). For this mode the spin wave has no transverse nodes and the transverse part of the magnetic potential is not sensitive to the detailed shape of the boundary. Therefore, in the adopted approximation, the fundamental branch of the spectrum coincides with the corresponding branch for a circular nanotube. The influence of ellipticity appears only for nonzero transverse modes, for which the functions $F(u,v,k_\perp)$ have a nontrivial dependence on the elliptic coordinates.

The circular nanotube is recovered as a limiting case when the two semiaxes become equal. In that limit, the Mathieu-function description passes into the Bessel-function description. Correspondingly, the even and odd elliptic modes become the two equivalent angular branches of the circular nanotube. For a genuinely elliptic cross-section this equivalence is removed: the reduction of rotational symmetry splits the transverse modes into different even and odd branches. Thus, ellipticity provides an additional geometrical mechanism for controlling the separation between transverse spin-wave modes. Let us consider this effect by keeping addends of the next order of magnitude by the cross-section eccentricity (which is equal to 1/cosh(u)). After applying asymptotics of the Mathieu functions and keeping the above-mentioned addends, one can – after a set of transformations – obtain a correction to the one-dimensional spectrum (14) that considers the cross-section ellipticity. The corresponding – more precise – expression for the transverse wavenumber looks as follows:

$$k_\perp = \frac{\pi n}{d} \pm \frac{e^{-(u_1+u_2)}}{2}\left[\frac{\pi n}{d} + \frac{k_\parallel^2 d}{\pi n}\right], \qquad (15)$$

for $m$=1, while the modes with higher values of $m$ receive no first-order wavenumber shift in this approximation – the corresponding corrections are of higher order of smallness. The upper and lower signs correspond to the two ellipticity-split branches of the circular $m$=1 doublet.

As one can see from the above relation, the leading ellipticity correction is proportional to $e^{-(u_1+u_2)}$. Since the usual geometrical eccentricity of the ellipse is

$$e_j^{\mathrm{geom}} = \frac{1}{\mathrm{ch}\, u_j} \simeq 2e^{-u_j},$$

the correction is of the order

$$e^{-(u_1+u_2)} \sim \frac{e_1^{\mathrm{geom}} e_2^{\mathrm{geom}}}{4}.$$

Thus, in the near-circular limit, ellipticity does not produce a first-order shift of all transverse eigenvalues. The fundamental mode $m=0, n=0$, for which $k_\perp = 0$, remains unchanged. The leading ellipticity effect on the spectrum is the splitting of the first angular doublet $m=1$, whereas higher angular modes acquire first-order changes mainly in their transverse magnetic-potential distribution. The ellipticity correction is proportional to $e^{-2u_j}$, i.e. to the first order of the boundary deformation and to the second order of the usual ellipse eccentricity.

## 7. RESULTS AND DISCUSSION

Let us analyze the physical consequences of the obtained expressions.

The spin-wave spectrum in the investigated nanotube is formed by two mechanisms of different origin. The first one is related to the thermoelectrically induced spin-polarized current, which affects the longitudinal propagation of the wave through the Zhang-Li spin-transfer torque. The second one is related to the elliptic geometry of the cross-section, which modifies the transverse quantization of the spin-wave modes. In the adopted approximation these two mechanisms enter the theory in a separated way: the temperature gradient changes the frequency and damping for a given pair of wave numbers $k_\parallel$, $k_\perp$, whereas ellipticity determines the allowed values of $k_\perp$.

For the positive-frequency branch, the real part of the frequency may be written in the form (8). Analogously to the previous paper [13] one can notice that the first term in this expression is the Doppler-type frequency shift produced by the adiabatic Zhang-Li torque ($\omega \to \omega_{\mathrm{eff}} = \omega - v_s k_\parallel$). Its sign is determined by the sign of $v_s k_\parallel$. Therefore, spin waves propagating along and against the thermoelectrically induced spin drift have different frequencies. This nonreciprocity is the same physical effect as in conducting ferromagnets with electric-current-induced spin-wave Doppler shift, but in the present system the current is generated by the temperature gradient rather than by an external voltage source.

The second term in $\omega_r$ is the ordinary dipole-exchange contribution. It contains the transverse wave number $k_\perp$, and this is where the ellipticity of the nanotube cross-section enters the frequency. Thus, ellipticity does not produce a separate additive term in the longitudinal dispersion law. Instead, it changes the allowed values of $k_\perp$, and through them changes the dipole-exchange part of the frequency. This is the principal difference between the present elliptic nanotube and the circular nanotube considered previously.

The imaginary part of the frequency has the form (9). Analogously to the previous paper by the authors [13], the first term in square brackets describes ordinary Gilbert damping. The second term is caused by the nonadiabatic Zhang-Li torque. Depending on the sign of $(\xi - \alpha_G)v_s k_\parallel$, this term may either compensate the intrinsic damping or increase it. Hence, the temperature gradient controls not only the phase of the spin wave but also its attenuation. Note that in the considered case of the elliptic nanotube, the threshold condition depends on the ellipticity through $k_\perp$.

The condition of spin-wave excitation (11) shows that spin-wave excitation is impossible at $k_\parallel = 0$ within the considered bulk Zhang-Li mechanism. The reason is that the current-induced torque is proportional to the spatial derivative of the magnetization along the current direction. For a longitudinally uniform excitation, this derivative vanishes. The expression (12) shows that higher transverse modes generally require different excitation thresholds than the fundamental mode, because of the dependence of $(\partial T/\partial z)_{\mathrm{cr}}$ on $k_\perp$. The special case $\xi = \alpha_G$ separates two regimes of thermoelectric control. At this point the current-dependent contribution to the imaginary part of the frequency vanishes.

The thermoelectrically induced spin current then produces only the Doppler shift of the real frequency and does not change the effective damping. For $\xi > \alpha_G$, a proper direction of the temperature gradient can reduce the damping and eventually lead to generation. For $\xi < \alpha_G$, the same direction of spin drift increases the attenuation; damping compensation would require reversing the sign of $v_s k_\parallel$.

Note that analogously to [13], the thermoelectric current within the adopted approximation modifies the frequency and damping of the spin wave but does not change the transverse wavenumber spectrum. Thus, the transverse mode structure of the nanotube is still determined primarily by its geometrical parameters, whereas the temperature gradient controls the propagation and attenuation of these modes along the nanotube axis.

Let us now consider the role of ellipticity. First, let us note that the ellipticity of the cross-section influences the spin-wave spectrum primarily through the transverse eigenvalues, while the longitudinal thermoelectric spin-transfer effects remain described by the dispersion relation obtained in the previous section. Even a weak ellipticity does not simply shift the whole transverse spectrum; it lowers the rotational symmetry and selectively splits/mixes the circular-tube modes.

The fundamental transverse mode, $k_\perp = 0$, is not affected by the ellipticity of the cross-section in the adopted approximation. Physically, this mode is nearly uniform over the nanotube wall, so it does not resolve the detailed transverse shape of the boundary. Therefore, the fundamental branch coincides with the corresponding branch of the circular nanotube. This result is important for comparison with the previous paper: the lowest spin-wave branch remains governed by the same thermoelectric Doppler shift and damping-control mechanisms as in the circular case.

The situation is different for nonzero transverse modes. In a circular nanotube the angular modes with the same $|\, m \,|$ are degenerate with respect to the choice of the angular basis, for example $\cos m\theta$ and $\sin m\theta$. In an elliptic nanotube this degeneracy is lifted because the cross-section no longer has continuous rotational symmetry. The transverse eigenfunctions are described by Mathieu functions rather than by Bessel-function angular harmonics, and the allowed values of $k_\perp$ are determined by an elliptic boundary-value problem. In the near-circular limit this effect appears as a small splitting of the circular-tube transverse modes.

For a thin elliptic nanotube close to a circular one, the leading quasi-one-dimensional spectrum is given by (14). This expression describes standing waves across the wall thickness and coincides with the circular-tube result. The next-order correction due to ellipticity is most important for the $m = 1$ doublet. In the near-circular confocal model, the split branches can be written as (15). Therefore, the leading spectral correction is first order in the boundary deformation parameter and second order in the usual geometrical eccentricity. (Modes with $m \neq 1$ acquire first-order corrections mainly in their spatial profile through admixture of neighboring angular harmonics, whereas their wavenumber shifts are of higher order in the ellipticity parameter.) This explains why the fundamental branch is robust, while higher transverse branches can be measurably shifted or split even for a weakly non-circular cross-section.

The frequency splitting corresponding to the two branches is approximately

$$\Delta\omega_r \simeq \gamma M_0 e^{-(u_1+u_2)} * \left[\frac{\pi n}{d} + \frac{k_\parallel^2 d}{\pi n}\right] \frac{\partial}{\partial k_\perp} \left[\sqrt{(\beta_0 + \alpha k^2)\left(\beta_0 + \alpha k^2 + 4\pi \frac{k_\perp^2}{k^2}\right)}\right],$$

$$\Delta\omega_i \simeq 2e^{-(u_1+u_2)} \left[\frac{\pi n}{d} + \frac{k_\parallel^2 d}{\pi n}\right] \frac{\partial \omega_i}{\partial k_\perp}.$$

This expression shows that the ellipticity-induced splitting is enhanced when the dipole-exchange frequency is sensitive to $k_\perp$. Consequently, the effect is weak for the fundamental mode and becomes more important for nonzero transverse modes, especially when the exchange term $\alpha k^2$ is comparable with or larger than the anisotropy contribution.

The obtained results are consistent with the general symmetry argument known for non-circular magnetic waveguides: lowering the rotational symmetry does not simply shift the entire spectrum uniformly, but separates modes that are equivalent in the circular geometry. In the present nanotube, this means that ellipticity provides an additional nanoscale control parameter. By changing the ratio of the semiaxes, one can tune the separation between transverse branches without changing the material, the wall thickness, or the applied temperature gradient.

Now, let us build and analyze graphical dependencies for the obtained results.

The first group of graphs (Fig. 2) show the real and imaginary parts of the frequency as well as their relation as functions of $k_\parallel$ and the temperature gradient for a fundamental mode (which coincides with a corresponding mode for the circular-tube case). These graphs are built for the $Ni_{80}Fe_{20}$ ferromagnet as the nanotube material (with its parameters taken from the papers [19-21]) in the absence of the external magnetic field ($H_0^{(e)} = 0$, $\beta_0 = \beta$).

As one can see from the Fig. 2, both real and imaginary parts of the frequency for the fundamental mode have pronounced dependencies on $\frac{\partial T}{\partial z}$ (everywhere except for the region where $k_\parallel$ is close to 0). Thus, the thermoelectrically induced spin-polarized current can noticeably modify both the real and imaginary parts of the spin-wave frequency in the considered parameter range. Analogously to the circular nanotube case [13], the minimal value of the real part of the frequency $\omega_r = \beta\gamma M_0 = 0.17$ GHz (for the used set of the ferromagnet parameters) is achieved when $k_\parallel = 0$. Dependence $\omega_r(k_\parallel)$ has a minimum at $k_\parallel = -v_s/2\alpha\gamma M_0$, dependence $\omega_i(k_\parallel)$ – at

$$k_\parallel = k_{||}^{(min)} = \frac{\kappa(\alpha_G - \xi)}{2\alpha_G \gamma M_0 \alpha} \frac{\partial T}{\partial z}$$

(becoming maximum when $\alpha k_\perp^2 - 2\pi < 0$). The dependence $\frac{\omega_i}{\omega_r}(k_\parallel, \frac{\partial T}{\partial z})$ for the fundamental mode has one local maximum and one local minimum at the points $k_{||} = \pm\sqrt{\beta/\alpha}$ (except for the case $\frac{\partial T}{\partial z} = 0$ for which $\frac{\omega_i}{\omega_r} = -\alpha_G = const$), asymptotically approaching the value $-\alpha_G$ for large (in absolute value) $k_{||}$ (both positive and negative).

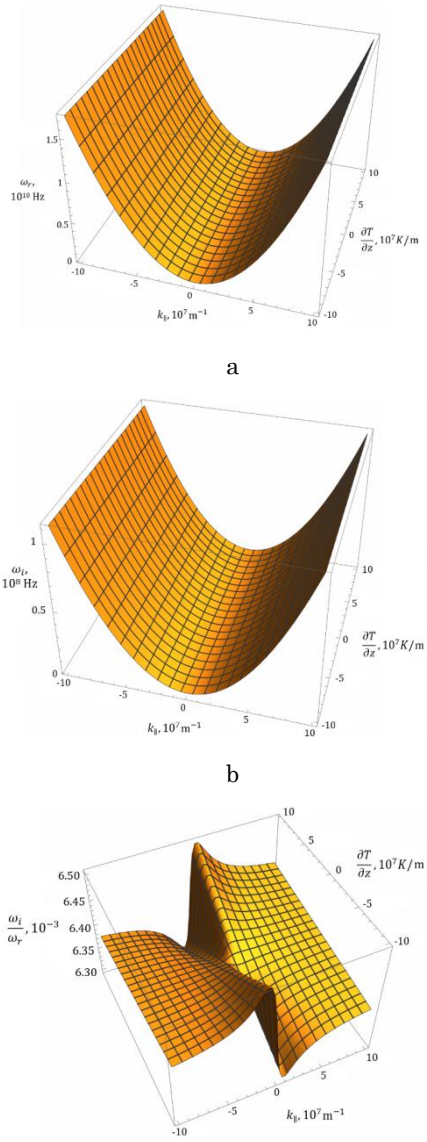

**Fig. 2** – Dependencies $\omega_r(k_\parallel, \frac{\partial T}{\partial z})$ (a), $\omega_i(k_\parallel, \frac{\partial T}{\partial z})$ (b) and $\frac{\omega_i}{\omega_r}(k_\parallel, \frac{\partial T}{\partial z})$ (c) for the fundamental mode (n=0). Nanotube material is considered to be $Ni_{80}Fe_{20}$

Dependencies $\omega_r(k_\parallel, \frac{\partial T}{\partial z})$, $\omega_i(k_\parallel, \frac{\partial T}{\partial z})$ and $\frac{\omega_i}{\omega_r}(k_\parallel, \frac{\partial T}{\partial z})$ for higher modes ($n$>0) with the quasi-one-dimensional transverse wavenumber spectrum (14) are analogous to the ones obtained previously for a circular nanotube [13] – thus, they are not given in this paper. They show the same regularities: dependencies for different generalized-radial modes (but on essentially different scales) have similar looks for both $\omega_r(k_\parallel, \frac{\partial T}{\partial z})$ and $\omega_i(k_\parallel, \frac{\partial T}{\partial z})$; dependencies on $\partial T/\partial z$ are pronounced for all modes; dependence $\frac{\omega_i}{\omega_r}(k_\parallel, \frac{\partial T}{\partial z})$ has similar form for all higher modes ($n$>0) – monotonous dependencies on $\partial T/\partial z$ (although the graphs have visual impression of saddle surfaces), dependencies on $k_\parallel$ contain single global minimum each – but they differ qualitatively from the dependence for the fundamental mode (n=0). The same regularities take place if the next-order corrections due to ellipticity are considered, but the index $m > 1$.

The next set of graphs illustrates corrections to the spectral characteristics of the investigated spin waves caused by the splitting of the $m = 1$ nonzero transverse modes that is caused by the cross-section ellipticity.

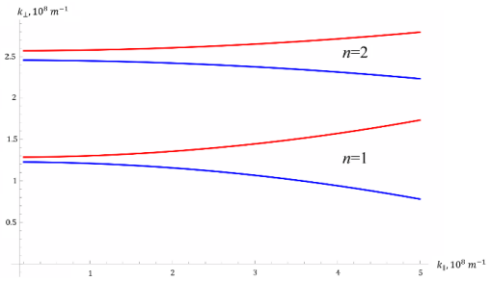


**Fig. 3** – Dependencies $k_\perp(k_{||})$ for the first and second angular-radial mode (the solution with m=1), with accounting for the first-order correction caused by the cross-section ellipticity. The nanotube geometric parameters are: $u_1$=1.5, $u_2$=1.6, $d$=25 nm. The red lines correspond to "+" sign in (15), the blue lines – to the "–" sign

Fig. 3 illustrates the dependence of the transverse wavenumber $k_\perp$ on the longitudinal one $k_{||}$ given by the relation (15) that takes into account the nanotube ellipticity in the first order of magnitude, for the first ($n$ = 1) and the second ($n$ = 2) angular-radial modes. The graph is built for a set of typical nanotube geometric parameters $u_1 = 1.5$, $u_2 = 1.6$, $d = 25$ nm (which correspond to $a_1$≈226 nm, $b_1$≈250 nm, $a_2$≈252 nm and $b_2$≈273 nm) in the interval of the longitudinal wavenumbers for which $k_{||} >> \pi n/d\sqrt{\mathrm{ch}2u_1 - 1}$ (so the relation $\mathrm{ch}2u_1 >> 1 + k_\perp^2/k_{||}^2$ fulfils and, thus, the dependence $k_\perp(k_{||})$ in the form (15) can be used).

As follows from the graph, the correction to the transverse wavenumber caused by the nanotube ellipticity can be essential even when the eccentricity is not large. The correction becomes more pronounced for large values of the longitudinal wave number, with the quadratic form of the corresponding dependence.

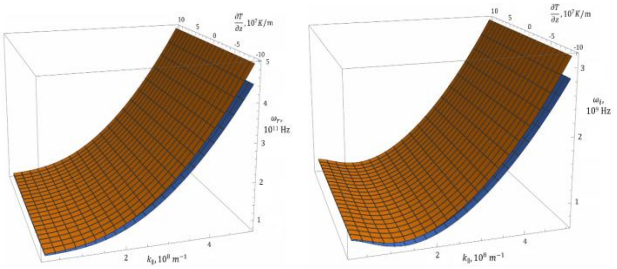

**Fig. 4** – Dependencies $\omega_r(k_\parallel, \frac{\partial T}{\partial z})$ (a) and $\omega_i(k_\parallel, \frac{\partial T}{\partial z})$ (b) for the first angular-radial mode (the solution with m=1), with accounting for the first-order correction caused by the cross-section ellipticity. Nanotube material is considered to be $Ni_{80}Fe_{20}$, and its geometric parameters are: $u_1$=1.5, $u_2$=1.6, d=25 nm. The orange surfaces correspond to "+" sign in (15), the blue surfaces – to the "–" sign

Fig. 4 illustrates the splitting of the $m = 1$ nonzero transverse modes (caused by the cross-section ellipticity) for both the real and imaginary parts of the spin wave

frequency. Geometrical parameters of nanotube are the same as for the Fig. 3 ($u_1 = 1.5$, $u_2 = 1.6$, $d = 25$ nm), and the nanotube material is $Ni_{80}Fe_{20}$ with the same parameters as for the Fig. 2. Interval of values of the longitudinal wavenumber is chosen so that $k_{||} >> \pi n/d\sqrt{\mathrm{ch}2u_1 - 1}$ on all the interval and, thus, using the dependence $k_\perp(k_{||})$ in the form (15) becomes correct.

As it can be seen from the figure, the modes' splitting can be pronounced for typical elliptic nanotubes not only in the transverse wavenumber spectrum, but also for both real and imaginary parts of the spin wave frequency. Each split branch has dependence on $k_\parallel$and $\nabla T$ similar to that of the corresponding unsplit transverse mode. Also, effects associated with the cross-section ellipticity are essentially more pronounced than the effects associated with the temperature gradient (for the chosen set of geometrical and material parameters). This, however, should be regarded as a parameter-dependent result rather than a universal hierarchy of the two effects.

Let us note that in the previous paper [13], the transverse wave number spectrum was obtained in the assumption $k_\parallel \ll k_{||}^{(min)} \sim d^{-1}$. In the current paper, on the other hand, the longitudinal wavenumber interval for the Fig. 4 covers much large values of $k_\parallel$ – because the transverse wavenumber spectrum has been obtained upon assumption that the relation $k_{||} >> \pi n/d\sqrt{\mathrm{ch}2u_1 - 1}$ fulfills. As the graphs on the Figure 4 are built for the values of the longitudinal wave number that are much higher than in the previous paper, weak local minimum for the dependence $\omega_i(k_\parallel)$ can be seen on the Fig. 4(b). Such minimum has been predicted (in the previous paper) to take place for the value

$$k_{||}^{(min)} \approx \frac{\kappa(\alpha_G - \xi)}{2\alpha_G \gamma M_0 \left(\alpha - \frac{2\pi}{k_\perp^2}\right)} \frac{\beta + \alpha k_\perp^2 + 2\pi}{\sqrt{(\beta + \alpha k_\perp^2)(\beta + \alpha k_\perp^2 + 4\pi)}} \frac{\partial T}{\partial z},$$

but was not graphically illustrated because of the limitation $k_\parallel \ll k_\perp$. Note that for the considered case of the elliptic nanotube, $k_{||}^{(min)}$ is split because of the splitting of the transverse wavenumber for the considered solution ($m$=1).

Numerical analysis shows that the dependence of the relation of the imaginary part of the frequency to the real one $\omega_i/\omega_r$ for the first radial-angular mode $n$=1 is very weak (with this relation being approximately equal to 0.0064) – thus, it won't be displayed on the graphs. However, this relation also shows pronounced (compared to the dependence $\frac{\omega_i}{\omega_r}(k_\parallel, \frac{\partial T}{\partial z})$ itself) splitting of the mode with $m = 1$. Moreover, this relation can have large value for the branch with the "+" or "–" sign in (15) depending on the sign of the temperature gradient $\partial T/\partial z$. At positive values of $\partial T/\partial z$, the relation for the "+" sign in 15 is more than the corresponding relation for the minus sign for the negative temperature gradient, vice versa.

Dependencies $\omega_r(u_1, \partial T/\partial z)$ and $\omega_i(u_1, \partial T/\partial z)$ are illustrated on the Fig. 5 (for $k_\parallel = 10^8$ m$^{-1}$ and the same ferromagnet). The nanotube thickness is $d = 25$ nm (with $u_2 - u_1 = 0.2$), and the internal surface coordinate $u_1$varies from 0.6 (minimal value for which the relation $k_{||} >> \pi n/d\sqrt{\mathrm{ch}2u_1 - 1}$ fulfils and, additionally, the ellipticity parameter $\mathrm{ch}^{-1}(u_1)\mathrm{ch}^{-1}(u_2) << 1$) to 2. The minimal value corresponds to the nanotube cross-section with the semiaxes $a_1 \approx 79$ nm, $b_1 \approx 147$ nm, $a_2 \approx 110$ nm and $b_2 \approx 166$ nm. For the maximum value $u_1 = 2$, the semiaxes are $a_1 \approx 111$ nm, $b_1 \approx 115$ nm, $a_2 \approx 136$ nm and $b_2 \approx 140$ nm. As in can be seen from the graphs, the frequency splitting becomes less pronounced for larger values of $k_\parallel$.

It should be noted that the negligible dependence of both the real and imaginary parts of the frequency on the temperature gradient $\partial T/\partial z$, observed in Figs. 4 and 5, is specific to the high-$k_\parallel$ range used for the $m = 1$ solution. This range is chosen to satisfy the applicability condition of Eq. (15), $k_{||} >> \pi n/d\sqrt{ch2u_1 - 1}$. For smaller longitudinal wavenumbers, which can still be considered when the transverse spectrum is taken in the quasi-one-dimensional form (14), the dependences $\omega_r(\partial T/\partial z)$and $\omega_i(\partial T/\partial z)$ remain pronounced, as they were in the case of the circular nanotube [13]. Thus, the apparent weakness of the thermoelectric effect in Figs. 4 and 5 should not be interpreted as a general property of the system, but rather as a consequence of the particular wavenumber interval required for applying the asymptotic ellipticity correction. The relative influence of the thermoelectric current on the dispersion law is expected to be most visible in the intermediate region of wave numbers, where the exchange and magnetostatic contributions are comparable.

Thus, the obtained results demonstrate the main new physical effect considered in this paper: the thermoelectrically induced spin-transfer torque controls the longitudinal propagation and effective damping, whereas the ellipticity of the cross-section acts as a transverse-mode splitting mechanism.

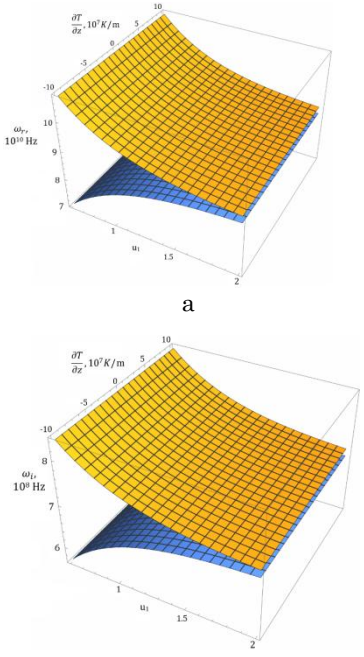


**Fig. 5** – Dependencies $\omega_r(u_1, \frac{\partial T}{\partial z})$ (a) and $\omega_i(u_1, \frac{\partial T}{\partial z})$ (b) for the first angular-radial mode (the solution with m=1), with accounting for the first-order correction caused by the cross-section ellipticity. Nanotube material is considered to be $Ni_{80}Fe_{20}$, its thickness d=25 nm (with $u_2 - u_1 = 0.2$), the longitudinal wavenumber $k_\parallel = 10^8$ m–1. The orange surfaces correspond to "+" sign in (15), the blue surfaces – to the "–" sign

## 8. CONCLUSIONS

Thus, a theory of linear dipole-exchange spin waves in a conducting ferromagnetic nanotube of elliptic cross-section subjected to an axial temperature gradient has been developed in the paper. The magnetization dynamics was described by the linearized Landau-Lifshitz-Gilbert equation with the Zhang-Li spin-transfer torque. The magnetic dipole-dipole interaction, the exchange interaction, the uniaxial anisotropy and the damping were taken into account in the magnetostatic approximation. The temperature gradient was considered as the source of a Seebeck-induced spin-polarized electric current flowing along the nanotube axis.

The equation for the magnetic potential of the spin wave was obtained in elliptic cylindrical coordinates. It was shown that the general structure of this equation is analogous to that for a circular nanotube, whereas the elliptic cross-section changes the transverse part of the problem. The transverse eigenfunctions are expressed through Mathieu functions, and the allowed transverse wavenumbers are determined by the boundary conditions at the inner and outer elliptic surfaces of the nanotube.

The dispersion relation for dipole-exchange spin waves was derived. The thermoelectrically induced spin current produces two effects. The adiabatic Zhang–Li term shifts the real part of the spin-wave frequency by a Doppler-type contribution proportional to $v_s k_\parallel$, where $v_s$ is the spin-drift velocity and $k_\parallel$ is the longitudinal wavenumber. The nonadiabatic term modifies the imaginary part of the frequency and, consequently, changes the effective damping. Depending on the direction and magnitude of the temperature gradient, this contribution may either enhance attenuation or compensate intrinsic Gilbert damping, or lead to a spin wave generation.

The condition for spin-wave excitation was obtained. It was shown that amplification is possible when the nonadiabatic spin-transfer contribution exceeds the intrinsic damping term. The corresponding threshold temperature gradient depends on the transverse mode through the transverse wavenumber $k_\perp$. Therefore, different transverse branches of the elliptic nanotube generally have different excitation thresholds.

The role of ellipticity was analyzed separately. The fundamental transverse mode, for which $k_\perp = 0$, is not affected by the ellipticity in the adopted approximation and coincides with the corresponding mode of a circular nanotube. Thus, the lowest spin-wave branch retains the same form as in the previously studied circular case. The influence of ellipticity appears for nonzero transverse modes, where it changes the transverse eigenfunctions and the transverse wavenumber spectrum.

After applying boundary condition, implicit relations for the transverse wavenumber spectrum has been obtained. It has been shown that the transverse quantization is determined by the same type of boundary-value problem as in a nanotube without thermoelectric driving, while the temperature gradient enters the final spin-wave spectrum through the dispersion relation. For a nanotube with a weakly elliptic cross-section, these relations were transformed into an explicit asymptotic expression for the leading ellipticity-induced correction to the transverse wavenumber. It was shown that ellipticity splits the $m = 1$ transverse doublet into two branches (here $m$ is the Mathieu functions index of the solution). The correction is first order in the boundary deformation parameter and second order in the usual geometrical eccentricity of the elliptic boundary. Higher angular modes do not acquire a first-order wavenumber shift in this approximation; their leading ellipticity effect appears mainly through changes of the transverse mode profile.

The results demonstrate that thermoelectric and geometrical effects act in different parts of the spin-wave problem. The temperature gradient controls longitudinal propagation and effective damping, while the elliptic cross-section acts as a transverse-mode splitting mechanism. Therefore, ellipticity provides an additional nanoscale degree of freedom for tuning spin-wave spectra in ferromagnetic nanotubes without changing the material parameters, wall thickness, or applied temperature gradient. This may be useful for the design of nanoscale magnonic waveguides, frequency-selective spin-wave filters, thermally controlled spin-wave amplifiers, and mode-selective elements in which different transverse branches are used as separate information channels. In particular, the possibility of controlling damping by a temperature gradient and controlling transverse-mode separation by ellipticity suggests a route toward compact spin-caloritronic devices where heat flow and cross-sectional geometry are combined to regulate spin-wave propagation, amplification, and spectral selectivity.

## DECLARATION OF COMPETING INTEREST

The authors declare that they have no known competing financial interests or personal relationships that could have appeared to influence the work reported in this paper.

## REFERENCES


1. M. Anderson, *J. Magn. Appl.* **5** No 2, 28 (2025) https://jourmag.org/index.php/jma/article/view/51.
2. A.V. Chumak, et al., *IEEE Trans. Magn.* **58** No 6, 1 (2022) https://doi.org/10.1109/TMAG.2022.3149664.
3. B. Flebus, D. Grundler, B. Rana, Y. Otani, I. Barsukov, A. Barman, J. Rao, *J. Phys.: Condens. Matter* **36** No 36, 363501 (2024) https://doi.org/10.1088/1361-648X/ad399c.
4. A.V. Chumak, V.I. Vasyuchka, A.A. Serga, B. Hillebrands, *Nature Phys.* **11**, 453 (2015) https://doi.org/10.1038/nphys3347.
5. Y. Ye, B. Geng, *Crit. Rev. Solid State Mater. Sci.* **37** No 2, 75 (2012) https://doi.org/10.1080/10408436.2011.613491.
6. R. Streubel, P. Fischer, F. Kronast, V.P. Kravchuk, D.D. Sheka, Y. Gaididei, O.G. Schmidt, D. Makarov, *J. Phys. D: Appl. Phys.* **49**, 363001 (2016) https://doi.org/10.1088/0022-3727/49/36/363001.
7. R. Streubel, J. Lee, D. Makarov, M.-Y. Im, D. Karnaushenko, L. Han, O.G. Schmidt, *Advanced Materials* **26** No 2, 316 (2014) https://doi.org/10.1002/adma.201303272.
8. J.A. Otálora, J.A. López-López, A.S. Núñez, P. Landeros,

*J. Phys.: Condens. Matter* **24**, 436007 (2012) https://doi.org/10.1088/0953-8984/24/43/436007
9. B. Singh, V.M.A. Salinas, M. Loeffler, et al., *npj Flex Electron* **9**, 89 (2025) https://doi.org/10.1038/s41528-025-00467-8.
10. L. Körber, M. Zimmermann, S. Wintz, et al., *Phys. Rev. B* **104** No 18, 184429 (2021) https://doi.org/10.1103/PhysRevB.104.184429.
11. Yu.I. Gorobets, V.V. Kulish, *Ukr. J. Phys.* **59** No 5, 541 (2014).
12. Yu.I. Gorobets, V.V. Kulish, *Open Phys.* **13**, 263 (2015) https://doi.org/10.1515/phys-2015-0033.
13. V.V. Kulish, S.I. Yeromin, *J. Thermoelectr.* No 2, 15 (2026) https://doi.org/10.63527/1607-8829-2026-2-15-39.
14. G. Yang, L. Sang, C. Zhang, N. Ye, A. Hamilton, M.S. Fuhrer, X. Wang, *Nature Rev. Phys.* **5** No 8, 466 (2023) https://doi.org/10.1038/s42254-023-00604-0.
15. H. Yu, S.D. Brechet, J.P. Ansermet, *Phys. Lett. A* **381** No 9, 825 (2017) https://doi.org/10.1016/j.physleta.2016.12.038.
16. S. Zhang, Z. Li, *Phys. Rev. Lett.* **93**, 127204 (2004) https://doi.org/10.1103/PhysRevLett.93.127204.
17. M. Krawczyk, D. Grundler, *J. Phys.: Condens. Matter* **26** No 12, 123202 (2014) https://doi.org/10.1088/0953-8984/26/12/123202
18. V. Vlaminck, M. Bailleul, *Science* **322** No 5900, 410 (2008) https://doi.org/10.1126/science.1162843.
19. H.Y. Liu, Z.K. Wang, H.S. Lim, S.C. Ng, M.H. Kuok, D.J. Lockwood, M.G. Cottam, K. Nielsch, U. Gösele, *J. Appl. Phys.* **98**, 046103 (2005) https://doi.org/10.1063/1.2009072.
20. F.K. Dejene, J. Flipse, B.J. van Wees, *Phys. Rev. B* **86**, 024436 (2012) https://doi.org/10.1103/PhysRevB.86.024436.
21. S. Lepadatu, et al., *Phys. Rev. B* **79**, 094402 (2009) https://doi.org/10.1103/PhysRevB.79.094402.

## Теорія спінових хвиль дипольного обміну у феромагнітній нанотрубці за наявності термоелектрично індукованого моменту переносу спіну. Випадок еліптичної нанотрубки

В.В. Куліш, С.І. Єрьомін

*Національний технічний університет України "Київський політехнічний інститут імені Ігоря Сікорського", 03056 Київ, Україна*

Розроблено теоретичну модель лінійних дипольно-обмінних спінових хвиль у провідній феромагнітній (феромагнетику легкої осі) нанотрубці еліптичного перерізу, підданій аксіальному градієнту температури. Температурний градієнт генерує термоелектричний спін-поляризований струм, дія якого на динаміку намагніченості описується членами крутного моменту Чжана-Лі. Обмінна взаємодія, диполь-дипольна взаємодія, одновісна анізотропія та затухання Гілберта враховуються в рамках лінеаризованого рівняння Ландау–Ліфшица–Гільберта та магнітостатичної апроксимації. Виведено відповідне дисперсійне співвідношення. Показано, що термічно індукований спіновий струм викликає доплерівський зсув дійсної частини частоти спінової хвилі та змінює ефективне затухання через неадіабатичний внесок спінового переносу. Отримано умову спін-хвильового збудження. Еліптичність поперечного перерізу впливає на спектр через поперечне квантування: основна мода залишається ідентичною моді круглої нанотрубки, тоді як ненульові поперечні моди описуються функціями Матьє в еліптичних циліндричних координатах. Неявний вираз для поперечного хвильового числа було знайдено та (для нанотрубки, близької до круглої) спрощено до явного асимптотичного виразу для еліптичної поправки до поперечного хвильового числа. Показано, що основним ефектом еліптичності є розщеплення поперечного дублета для першої моди, тоді як вищі моди не отримують зсуву хвильового числа першого порядку в цьому наближенні. Результати демонструють, що температурний градієнт контролює поздовжнє поширення та демпфування, тоді як еліптичність забезпечує додатковий геометричний механізм для налаштування мод поперечних спінових хвиль у нанорозмірних магнонних та спін-калоритронних пристроях.

**Ключові слова:** Спінова хвиля, Наномагнетизм, Теорія дипольного обміну, Розщеплення мод, Термоелектрика, Перенесення спіну.